Modulation of the Oligomerization of Isolated Ryanodine Receptors by their Functional States

Xiao-Fang Hu,* Xin Liang,* Ke-Ying Chen,* Hong Xie,† Yuhong Xu,‡ Pei-Hong Zhu,† and Jun Hu*§

*Bio-X Life Science Research Center, College of Life Sciences and Biotechnology, Shanghai Jiao Tong University, Shanghai, China; †Key Laboratory of Neuroscience, Shanghai Institutes for Biological Sciences, Chinese Academy of Sciences, Shanghai, China; ‡School of Pharmacy, Shanghai Jiao Tong University, Shanghai, China; and §Shanghai Institute of Applied Physics, Chinese Academy of Sciences, Shanghai, China

ABSTRACT The calcium release channels/ryanodine receptors (RyRs) usually form two-dimensional regular lattices in the endoplasmic/sarcoplasmic reticulum membranes. However, the function and modulation of the interaction between neighboring RyRs are still unknown. Here, with an in vitro aqueous system, we demonstrate that the interaction between RyRs isolated from skeletal muscle (RyR1s) is modulated by their functional states by using photon correlation spectroscopy and [^{3}H]ryanodine binding assay. High level of oligomerization is observed for resting closed RyR1s with nanomolar Ca^{2+} in solution. Activation of RyR1s by micromolar Ca^{2+} or/and millimolar AMP leads to the de-oligomerization of RyR1s. The oligomerization of RyR1s remains at high level when RyR1s are stabilized at closed state by Mg^{2+}. The modulation of RyR1-RyR1 interaction by the functional state is also observed under near-physiological conditions, suggesting that the interaction between arrayed RyR1s would be dynamically modulated during excitation-contraction coupling. These findings provide exciting new information to understand the function and operating mechanism of RyR arrays.

INTRODUCTION

Ryanodine receptors (RyRs) belong to the class of ion channels mediating Ca^{2+} release from endoplasmic/sarcoplasmic reticulum (SR), and play a pivotal role in intracellular Ca^{2+} signaling processes, such as excitation-contraction coupling (E-C coupling), in muscle cells (1–5). Three different isoforms of RyRs have been identified in mammals, designated as skeletal (RyR1), cardiac (RyR2), and brain (RyR3) (1,2). Intriguingly, RyRs in intact muscle cells are almost exclusively found to be assembled into two-dimensional paracrystalline arrays in SR membrane (6–9). The interaction between neighboring RyRs may play an essential role in the activation and termination of Ca^{2+} release during E-C coupling. The ''coupled gating'' of RyRs has been observed in vitro for reconstituted RyRs isolated from both skeletal and cardiac muscle cells (10,11). Recently, by analysis of the quantal nature of Ca^{2+} sparks, the elementary Ca^{2+} release events, Cheng et al. have demonstrated that the gating kinetics of multiple RyRs is reshaped by the array-based interaction between these channels (12–14). However, the nature of the underlying RyR-RyR interaction and its modulation during E-C coupling is still unknown.

Clearly, the investigation of the modulation of RyR-RyR interaction by functional channel state would provide exciting new information, shedding light on the function and operating mechanism of RyR arrays. The potential RyR-RyR interacting site is found on the conserved, clamplike subdomains located at the four corners of the cytoplasmic region of the channel protein (6–9,15). The profound conformational changes of these domains accompanying the activation of RyR (16–18) suggest the potential of the channel's functional states to modulate the interaction between RyRs. Examination of RyR-RyR protein interaction in vivo would be extremely difficult given present techniques. Recently, by electron microscopy study it has been shown that isolated RyR1s in aqueous medium could self-assemble into a two-dimensional array, with similar dimensions to those observed in native SR membrane (15). Thus, it is plausible to work with such a simple system to look at the basic features of the interaction between RyRs, as modulated by their functional states.

In the present work, the modulation of RyR1-RyR1 interaction by their functional states was studied by examining the oligomerization and de-oligomerization of isolated RyR1s in aqueous medium accompanying their activation by endogenous activators, Ca^{2+} and AMP, and inhibitor Mg^{2+}. Photon correlation spectroscopy (PCS), also referred to dynamic light scattering, was employed for its high sensitivity to the aggregation state of proteins in solution (19–22). The functional state of isolated RyR1s in the presence of Ca^{2+}/AMP/Mg^{2+} was examined by [^{3}H]ryanodine binding assay. By analysis of the correlation between RyR1 oligomerization and RyR1 activity, we demonstrate that the interaction between RyR1s decreases with the activation of the channels. These findings provide new insight for understanding the modulation and function of the interaction between arrayed RyRs during E-C coupling.

Submitted April 26, 2005, and accepted for publication May 27, 2005.

Address reprint requests to Prof. Jun Hu, Bio-X Life Science Research Center, College of Life Sciences and Biotechnology, Shanghai Jiao Tong University, 1954 Hua-Shan Road, Shanghai 200030, China. Tel.: 86-21-640-77360; Fax: 86-21-644-72577; E-mail: jhu@sjtu.edu.cn.

0006-3495/05/09/1692/08 $2.00

doi: 10.1529/biophysj.105.065409

MATERIALS AND METHODS

Isolation and purification of RyR1

The isolation and purification of RyR1 from rabbit skeletal muscle were as described previously (22–24). All the reagents were purchased from Sigma-Aldrich (St. Louis, MO). In brief, the heavy sarcoplasmic reticulum (HSR) vesicles were prepared by sucrose step-gradient centrifugation (20%:35%:40%, w/w). Then, the HSR vesicles were solubilized with 3-[(3-cholamidopropyl) dimethylammonio]-1-propanesulfonate (CHAPS). The solubilized proteins were fractionated by centrifugation on a 6–20% linear sucrose gradient. The protein composition of 1 ml fractions was monitored by SDS-polyacrylamide gel electrophoresis and identified by Western blot analysis. The fraction containing highly purified RyR1 was used for this study. The buffer for storing the isolated RyR1s contained 1 M KCl, 20 mM K-PIPES, 100 μM EGTA, 1 mM dithiothreitol, 1 mM diisopropylfuorophosphate, pH 7.1, with 10 mM CHAPS, and 3 mg/ml phosphatidylcholine (PC), ~17% sucrose. The protein concentration was ~100 μg/ml. The purity of RyR1 was ~90%, as estimated from silver-stained polyacrylamide gel.

[^{3}H]Ryanodine binding assay

These experiments were carried out according to the method of Pessah et al. (25). HSR vesicles (0.25 mg protein/ml) or isolated RyR1s (2 μg/ml) were incubated at 34°C for 4.5 h, with various concentrations of free Ca^{2+}, Mg^{2+}, and AMP in binding buffer containing 20 mM PIPES, 100 μM EGTA, and 130 mM KCl-20 mM NaCl, pH 7.1, and radioligand: 1 nM [^{3}H]ryanodine and 14 nM ryanodine (for HSR) or 2 nM [^{3}H]ryanodine and 3 nM ryanodine (for isolated RyR1s).The total Ca^{2+}, Mg^{2+}, and AMP necessary for obtaining the desired free concentration in binding buffer was calculated by the new version of a computer program, Winmaxc (26). The binding reaction was quenched by rapid filtration through Whatman GF/B filters (Whatman, Florham Park, NJ) mounted on a 48-well Brandel Cell Harvester (Brandel, Gaithersburg, MD). The filters were rinsed three times with ice-cold wash buffer, put into scintillation vials and shaken overnight with scintillation fluid, and bound [^{3}H]ryanodine determined by scintillation counting (Model LS 6000IC, Beckman-Coulter, Fullerton, CA).

Photon correlation spectroscopy

Theory

In a typical light-scattering experiment, a laser beam impinges on a solution and the scattered light is recorded by a photomultiplier. The spatial resolution of the experiment is defined by the scattered vector q, whose magnitude is given by the Bragg formula as

$$|q| = \frac{4\pi n}{\lambda}\sin\left(\frac{\theta}{2}\right), \tag{1}$$

where λ denotes the wavelength of the scattered light, n is the refractive index of the solution, and θ is the scattering angle.

In a PCS experiment, the fluctuations of the scattered light due to the Brownian motion of the particles are analyzed in terms of an autocorrelation function, which is proportional to the distribution of relaxation time, τ, and scattering amplitudes of the examined components (20),

$$g^{(1)}(\tau) = \int_0^\infty m_\Gamma^2 P(q,\Gamma)\, G(\Gamma)\, e^{-\Gamma\tau} d\Gamma, \tag{2}$$

where m_Γ is the particle mass, $P(q, \Gamma)$ is the particle scattering factor, and $G(\Gamma)$ is the normalized number distribution function for the decay constant Γ. $\Gamma = q^2 D_T$. D_T is the translational diffusion coefficient. If the particles are small compared with the employed wavelength, D_T can be determined through Laplace inversion of the autocorrelation function.

From D_T, the apparent hydrodynamic diameter (D_h, Z-average) of the particles are calculated according to the Stokes-Einstein equation

$$D_h = \frac{k_B T}{3\pi\eta D}, \tag{3}$$

where k_B denotes the Boltzmann constant, T the absolute temperature, and η the viscosity of the solvent.

In the case of large, asymmetric particles, rational motions also contribute to the autocorrelation function. The magnitude of this effect can be roughly estimated according to Linsay et al. (27,28).

Experimental setup

PCS measurements were performed on a Zetasizer 3000HS$_A$ (Malvern Instruments, Malvern, Worcestershire, UK) with an He-Ne laser, operating at a 633-nm wavelength. The scattering angle for size analysis was fixed at 90 degrees. All measurements were carried out at 20°C. Solvent and particle refractive indexes were set to 1.330 and 1.520, respectively. Solvent viscosity was set to 1.00 for analysis at 20°C. CONTIN was chosen as the analysis method due to its suitability for describing smooth distributions.

Sample preparation for PCS

To prepare samples for PCS measurement, the original purified RyR1 in 1 M KCl storage buffer was diluted to a final solution containing 130 mM K^+-20 mM Na^+. The diluted RyR1 samples also contained 0.3 mg/ml PC, 1 mM CHAPS, 0.1 mM dithiothreitol, 100 μM EGTA, 20 mM PIPES, 10 μg/ml RyR1, and the desired concentration of Ca^{2+} $[Ca^{2+}]_f$/$[Mg^{2+}]_f$/AMP, pH 7.1. After dilution, all of the RyR1 samples were immediately mixed (300 rpm) on a Thermomixer (Eppendorf, Westbury, NY) at 20°C for 30 min before PCS measurement. A control sample, which contained 1 mM CHAPS and 0.3 mg/ml PC in the absence of RyR1, was also examined (22). It was found that PC and CHAPS formed ~26-nm homogeneous particles independent of the presence of the Ca^{2+}, Mg^{2+}, and AMP used in this work.

RESULTS

Identification of purified RyR1

First, the purity and activity of the purified RyR1 sample were identified. Fig. 1 *A* shows the SDS-PAGE analysis of a purified RyR1 sample. Two bands, indicated by arrows, were identified as of RyR1 origin by Western blotting with anti-RyR antibody 34C. The first band is consistent with the intact RyR1 monomer, whereas the second band represents a cleaved RyR1 fragment (23,29). Obviously, only a small amount of RyR1 underwent proteolysis during purification. Besides these two bands, only one contaminating band between 97 KDa and 116 KDa, generated by Ca^{2+}-ATPase (23,29), was observed. The purity of intact RyR1 was ~90%. To test if purified RyR1 retains activity, Ca^{2+}-dependence of [^{3}H]ryanodine binding was examined. Similar to HSR, a bell-shaped Ca^{2+} dependence of [^{3}H]ryanodine binding was obtained for purified RyR1, with a peak binding at ~10 μM free Ca^{2+} ($[Ca^{2+}]_f$) (Fig. 1 *B*), and consistent with previous results (2,4,30). In addition, [^{3}H]ryanodine binding by purified RyR1 maintained its response to activation by AMP and inhibition by Mg^{2+} (data not shown). Given the broader [^{3}H]ryanodine binding curve for purified RyR1 relative to HSR, it is likely that other proteins in HSR contribute to the Ca^{2+} responsiveness of the channel.

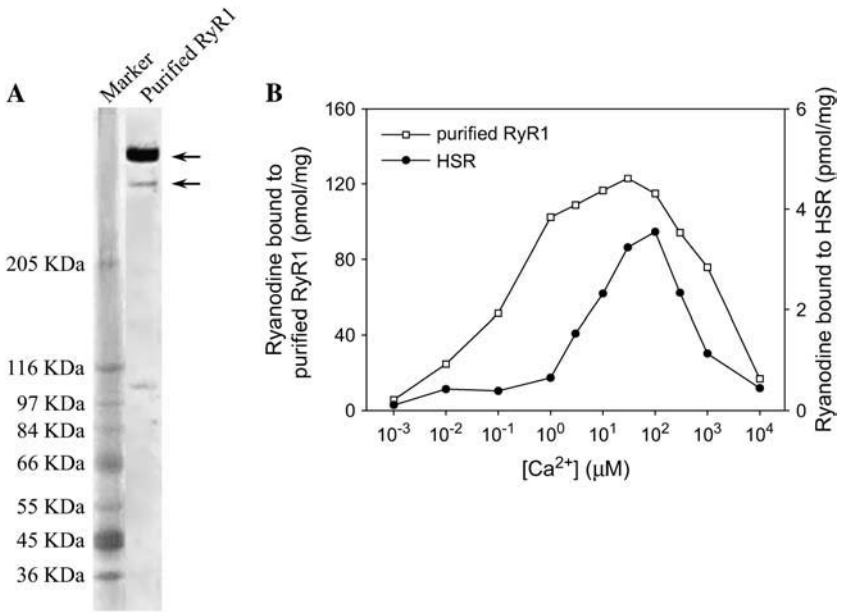

FIGURE 1 Identification of purified RyR1. (*A*) Silver-stained polyacrylamide gel (3–20%) of purified RyR1 preparations (1 μg). (*B*) Ca^{2+} dependence of [^{3}H]ryanodine binding to HSR vesicles and purified RyR1 in binding buffer with 130 mM KCl-20 mM NaCl. Each assay was performed on duplicate samples and repeated twice.

Modulation of RyR1 oligomerization by Ca^{2+}

Previous studies have demonstrated that purified RyR1 could oligomerize in aqueous solution near physiological ionic strength (15,22). To investigate the modulation of RyR1-RyR1 interaction by Ca^{2+}, the oligomerization state of RyR1s in the medium containing 130 mM KCl-20 mM NaCl with different concentration of Ca^{2+} was examined by PCS.

The representative size distributions of RyR1 samples measured in the presence of resting 0.1 μM $[Ca^{2+}]_f$ and activating 50 μM $[Ca^{2+}]_f$ are presented in Fig. 2 *A*. At 0.1 μM $[Ca^{2+}]_f$, three peaks were usually observed (Fig. 2 *A*, *left panel*). As indicated in our previous article (22), the peak at ~30 nm represents the distribution of PC-CHAPS particles (~26 nm) and the monodisperse RyR1s. Besides this peak, two peaks at ~200 nm and ~700 nm were usually observed, reflecting the high oligomerization state of RyR1s. Sometimes, we only observed two peaks. Besides the peak at ~30 nm, the second peak is broad to cover 100–1000 nm. In the presence of 50 μM $[Ca^{2+}]_f$, the oligomerization degree was decreased. Aside from the 30-nm peak, only one additional peak at 200–300 nm was usually observed (Fig. 2 *A*, *right panel*).

The average hydrodynamic diameter (Z-average) obtained from PCS measurement provides a way to semi-quantify the oligomerization state of RyR1 samples, although this parameter does not represent the actual dimensions of RyR1 oligomers (19). With this parameter, we quantitatively analyzed the oligomerization level of RyR1 samples accompanying the increase/decrease of $[Ca^{2+}]_f$ (Fig. 2 *B*). When $[Ca^{2+}]_f$ was increased from 0.1 μM to 50 μM, the Z-average decreased from 65.4 ± 3.0 nm ($n = 12$) to 49.6 ± 1.2 nm ($n = 8$). To test if such Ca^{2+}-modulation of RyR1 oligomerization is reversible, EGTA was added to the sample to reduce $[Ca^{2+}]_f$ from 50 μM to ~0.1 μM. After the addition of EGTA, the Z-average gradually increased and reached plateau equivalent to control levels after ~45 min (Fig. 2 *B*). These results demonstrate that the decreased oligomerization of RyR1s in the presence of activating μM $[Ca^{2+}]_f$ could be completely reversed after a decrease in $[Ca^{2+}]_f$.

Then the $[Ca^{2+}]_f$ dependence of oligomerization of RyR1s was examined in detail (Fig. 3). To investigate the correlation between Ca^{2+}-dependent RyR1 oligomerization and Ca^{2+}-dependent RyR1 activity, the Ca^{2+} dependence of [^{3}H]ryanodine binding of isolated RyR1s was also determined. As shown in Fig. 3, a close correlation between RyR1 de-oligomerization and RyR1 activation was observed. At 0.1 μM $[Ca^{2+}]_f$, the Z-average began to decrease with the slight activation of RyR1s, as reflected by the small increase in [^{3}H]ryanodine binding. When $[Ca^{2+}]_f$ was increased from 0.1 μM to 1 μM, the Z-average decreased sharply from 65.4 ± 3.0 nm ($n = 10$) to 52.9 ± 1.8 nm ($n = 10$), in close correspondence with the acute increase of RyR1 [^{3}H]ryanodine binding activity. In the range of 1–100 μM $[Ca^{2+}]_f$, the Z-average decreased very slowly. The Hill constants and coefficients were derived from our Ca^{2+} dependence of [^{3}H]ryanodine binding curves, as described by Meissner et al. (31). As calculated with these parameters, the percentage of RyR1 bound with Ca^{2+} at their activation sites slowly increased from 85.9% at 1 μM $[Ca^{2+}]_f$ to 99.7% at 100 μM $[Ca^{2+}]_f$. Accordingly, the Z-average decreased slowly from 52.9 ± 1.8 nm ($n = 10$) at 1 μM $[Ca^{2+}]_f$ to 48.6 ± 1.6 nm ($n = 10$) at 100 μM $[Ca^{2+}]_f$. Such close correlation between RyR1 de-oligomerization and RyR1 activation by Ca^{2+} suggests that RyR1 oligomerization is related to RyR1 functional states.

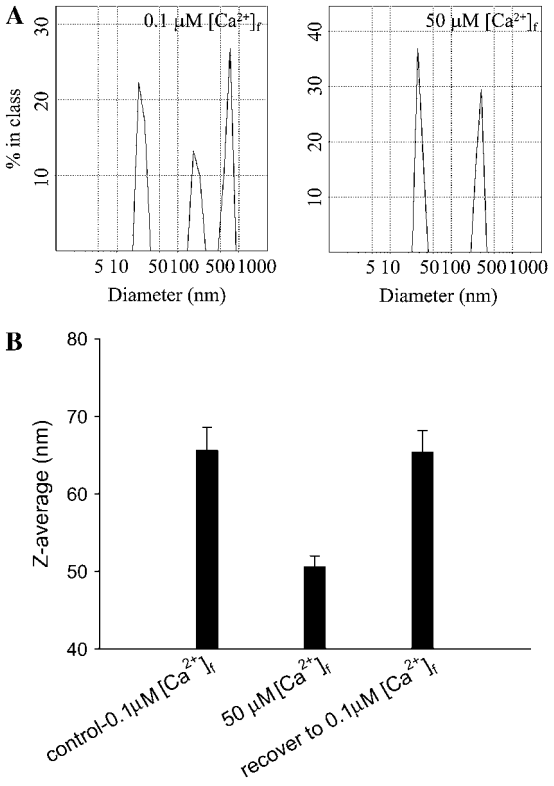

FIGURE 2 Modulation of RyR1 oligomerization by Ca^{2+}. (*A*) Representative size distributions of RyR1 samples measured by PCS in the presence of 0.1 μM $[Ca^{2+}]_f$ (*left panel*) and 50 μM $[Ca^{2+}]_f$ (*right panel*). All the samples contained 10 μg/ml RyR1. Similar results were obtained in other 10 experiments. (*B*) The reversibility of Ca^{2+}-modulated RyR1 oligomerization. Statistical representation of the Z-average of RyR1 sample before and after the decrease of $[Ca^{2+}]_f$. The Z-average obtained in the presence of 0.1 μM $[Ca^{2+}]_f$ was used as control. All the samples contained 10 μg/ml RyR1. Data are presented as mean ± SD for 3–5 independent experiments.

Modulation of RyR1 oligomerization by AMP

ATP, another potent activator of RyR1, exists in resting skeletal muscle fibers at a concentration of 6–8 mM. In this study, we investigated the effect of AMP, an ATP analog, on RyR1 oligomerization. Fig. 4 *A* shows the results when RyR1s were activated by 5 mM AMP or/and 50 μM Ca^{2+}. In the absence of Ca^{2+}/AMP, the Z-average of 10 μg/ml RyR1 sample was 67.8 ± 3.0 nm ($n = 12$) when RyR1s were at their closed state as reflected by the low ryanodine bound. In the presence of 5 mM AMP, the [^{3}H]ryanodine bound was increased to 53.9 ± 1.8 pmol/mg protein ($n = 3$), and the Z-average was decreased to 51.1 ± 1.6 nm ($n = 8$), similar to that obtained with 50 μM $[Ca^{2+}]_f$ (49.6 ± 1.2 nm ($n = 8$)). Thus, the activation of RyR1s by AMP was also accompanied by the de-oligomerization of RyR1s.

When RyR1 was fully activated by the co-presence of 50 μM $[Ca^{2+}]_f$ and 5 mM AMP, the [^{3}H]ryanodine bound further increased to 124.8 ± 9.7 pmol/mg protein ($n = 3$), and the Z-average was further decreased to 38.1 ± 0.8 nm ($n = 12$) (Fig. 4 *A*). This indicates the additive effect of activating Ca^{2+} and AMP on the de-oligomerization of RyR1s. Such effect was further investigated by measuring the Ca^{2+}-dependent oligomerization of RyR1s in the presence of 5 mM AMP. As shown in Fig. 4 *B*, compared to the curve obtained without AMP, the AMP did not change the overall tendency, but did lower the Z-average levels at all measured Ca^{2+} concentrations.

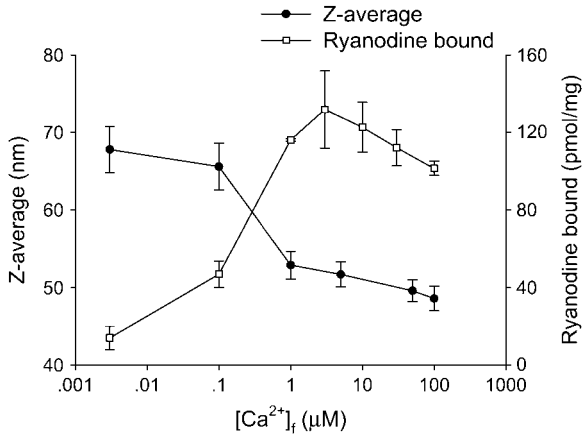

FIGURE 3 Correlation of Ca^{2+} dependence of the Z-average and Ca^{2+} dependence of [^{3}H]ryanodine binding for purified RyR1. All experiments were performed in solution containing 130 mM K^+-20 mM Na^+. [^{3}H]ryanodine binding assay was performed on duplicate samples and repeated three times. The samples for PCS measurements contained 10 μg/ml RyR1. Data are presented as mean ± SD for 3–5 independent experiments.

Modulation of RyR1 oligomerization by Mg^{2+}

Mg^{2+} is an inhibitor of RyR. It also binds to Ca^{2+} activation sites, but inhibiting RyR1 activity in doing so (4,30). Mg^{2+} modulation of RyR1 oligomerization was also investigated and the result was shown in Fig. 5. For comparison, the Ca^{2+} dependence of Z-average was also presented in this figure. Evidently, there was significant difference between the effects of Ca^{2+} and Mg^{2+} on RyR1 oligomerization. In contrast to the continuous decrease of Z-average when $[Ca^{2+}]_f$ was increased from 3 nM to 100 μM, the Z-average value remained at a high level (~68 nm) with $[Mg^{2+}]_f$ up to 500 μM. These observations indicate that RyR1s retain the high oligomerization state when RyR1s are ensured at their closed state by Mg^{2+}.

Modulation of RyR1 oligomerization by Ca^{2+} under near-physiological conditions

Under physiological conditions in resting skeletal muscle fibers, Mg^{2+} and ATP are present at 1 mM and 6–8 mM concentrations, respectively (32). During E-C coupling, the concentration of Ca^{2+} near RyR1 arrays would increase rapidly. To investigate the modulation of RyR1-RyR1 interaction during this process, the Ca^{2+}-dependence of Z-average and

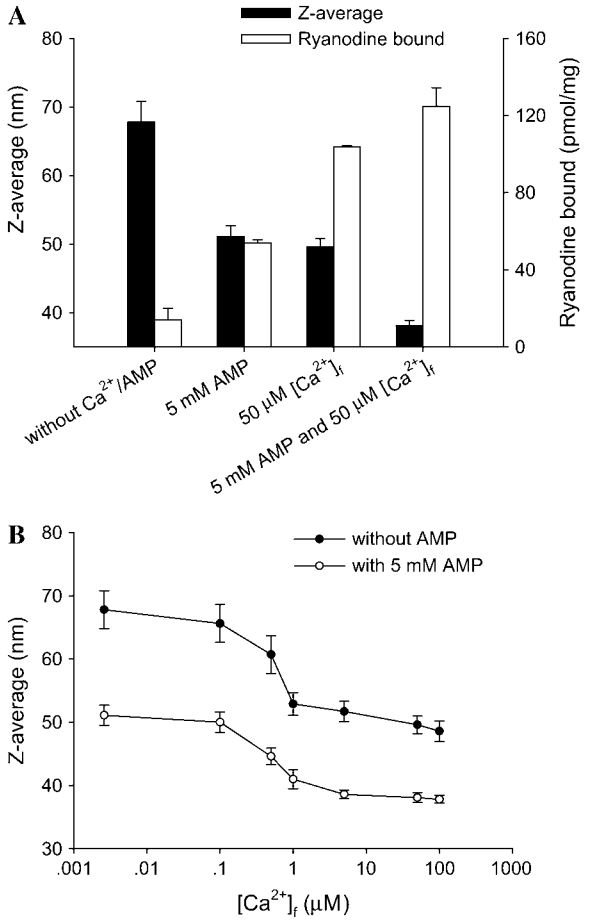

FIGURE 4 Modulation of RyR1 oligomerization by AMP. (*A*) Correlation of Z-average and ryanodine binding with the activation of RyR1s by 5 mM AMP or/and 50 μM $[Ca^{2+}]_f$. (*B*) Effect of 5 mM AMP on the Ca^{2+} dependence of the Z-average. All experiments were performed in solution containing 130 mM K^+-20 mM Na^+. [^{3}H]ryanodine binding assay was performed on duplicate samples and repeated three times. The samples for PCS measurements contained 10 μg/ml RyR1. Data are presented as mean ± SD for 3–5 independent experiments.

Ca^{2+}-dependence of [^{3}H]ryanodine binding were both examined (Fig. 6). In the presence of up to 0.1 μM $[Ca^{2+}]_f$, RyR1s retained a high level of oligomerization when RyR1s were in their closed state, as determined by [^{3}H]ryanodine binding. When RyR1 was activated by further increasing $[Ca^{2+}]_f$, the Z-average quickly decreased to lower levels, indicating that de-oligomerization of RyR1s also accompanied the activation of RyR1s under near-physiological aqueous conditions.

DISCUSSION

Modulation of RyR1-RyR1 interaction by the functional states of RyR1s

In the present work, Ca^{2+}, AMP, and Mg^{2+} modulation of RyR1 oligomerization was systematically investigated and

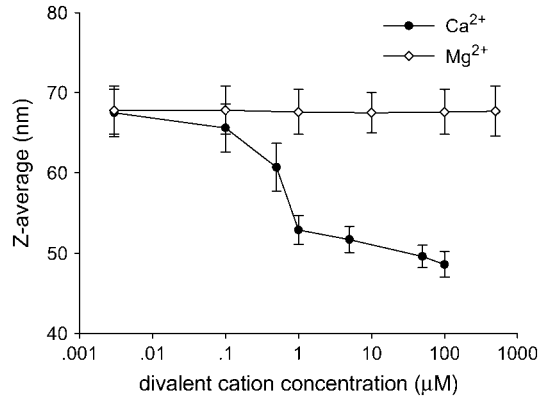

FIGURE 5 Comparison of Mg^{2+} and Ca^{2+} dependence of the Z-average. All experiments were performed in solution containing 130 mM K^+-20 mM Na^+. All samples contained 10 μg/ml RyR1. Data are presented as mean ± SD for 3–5 independent experiments.

the basic rules were obtained. Obviously, several lines of evidence support that the interaction between RyR1s is closely correlated with their functional states.

First, RyR1-RyR1 interaction decreases accompanying the activation of the channels. Strong oligomerization is observed for closed RyR1s with nanomolar Ca^{2+} in solution. Activation of RyR1s by 50 μM $[Ca^{2+}]_f$ or 5 mM AMP leads to the de-oligomerization of RyR1s (Fig. 2 and Fig. 4 *A*).

Second, the decreased degree of RyR1-RyR1 interaction is closely correlated with the increased level of RyR1 activity. In the presence of Ca^{2+}, the decrease in Z-average is always closely correlated with the Ca^{2+}-activation level of RyR1s (Fig. 3). In the co-presence of Ca^{2+} and AMP, Z-average decreases to lower level with the additive activation of RyR1s by Ca^{2+} and AMP (Fig. 4, *A* and *B*).

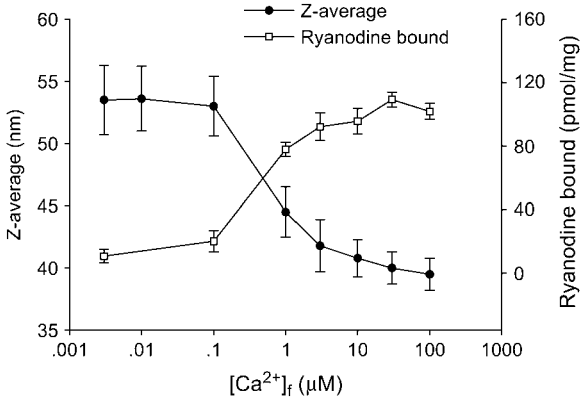

FIGURE 6 Correlation of Ca^{2+} dependence of the Z-average and Ca^{2+} dependence of [^{3}H]ryanodine binding obtained in 130 mM K^+-20 mM Na^+ solutions with 1 mM Mg^{2+} and 5 mM AMP. [^{3}H]ryanodine binding assay was performed on duplicate samples and repeated three times. All samples for PCS measurements contained 10 μg/ml RyR1. Data are presented as mean ± SD for 3–5 independent experiments.

Third, RyR1-RyR1 interaction remains at a high level when RyR1s are stabilized at a closed state by Mg^{2+}. Functional studies have indicated that Ca^{2+} binds to its activation sites with a *K*d of ~1 μM, whereas Mg^{2+} binds to these sites with a *K*d of 20~50 μM by inhibiting RyR1 activity (4,30). As shown in Fig. 5, the increase of Mg^{2+} from low nM to 500 μM, which stabilizes RyR1 in its closed state, does not induce the de-oligomerization of RyR1. The significant difference between the effects of Ca^{2+} and Mg^{2+} on RyR1 oligomerization further indicates that the de-oligomerization of RyR1 is correlated with the activation of RyR1.

Thus, from the analysis of the correlation between RyR1 oligomerization and RyR1 activity, we demonstrate that the RyR1-RyR1 interaction is potently modulated by their functional states. Strong interaction exists between resting closed RyR1s. The activation of RyR1s leads to the decrease in RyR1-RyR1 interaction.

RyR1 conformational relevance of such modulation

From the intuitive point of view, such modulation of RyR1-RyR1 interaction is related to the conformational change(s) of RyR1. Using techniques of electron microscopy, it has been demonstrated that with activation of RyR1, both transmembrane domain and cytoplasmic domain undergo conformational changes (16,17). A profound conformational change is found on the clamp regions, located on the four corners of the cytoplasmic domain of the channel (16,17). It should be noted that this clamp region is the domain at which RyR1s interact with each other to form regular lattices in SR membrane or in solution (6–9,15). The clamp regions undergo a stepwise conformational change with the transient/full activation of RyR1 (17). Correspondingly, we found in our work that RyR1-RyR1 interactions decreased step by step with the transient activation of RyR1 by 50 μM Ca^{2+}, and full activation of RyR1 by 50 μM Ca^{2+} and 5 mM AMP (Fig. 4 *A*). Such close correlation between RyR1-RyR1 interaction, as measured by PCS, and conformational change in clamp regions suggests that the clamp regions are possibly the structural basis for the modulation of the interaction between RyR1s by their functional states. Although it would be extremely interesting, mechanistically, to know whether de-oligomerization occurs before or after RyR1 channel opening, the techniques used here are not kinetically sensitive enough to distinguish between these two possibilities.

Implication for function and operating mechanism of RyR arrays

The functional state modulated RyR1-RyR1 interaction is also observed under near-physiological conditions (Fig. 6), suggesting that the interaction between arrayed RyR1s would be dynamically modulated during E-C coupling. Such modulation provides exciting new information to understand the function and operating mechanism of RyR arrays.

First, the strong interaction between closed RyR1s provides a novel stability mechanism for arrayed RyR1s at resting conditions. By forming a close contact, every RyR1 can be ensured at a quiescent closed state by the stabilization from neighboring RyR1s. In skeletal muscle, some RyR1s in two-dimensional array are respectively apposed to a dihydropyridine receptor (DHPR) tetrad (7,8). Although DHPR tetrads may exert inhibition on the apposing RyR1s (33–36), those RyR1s without the apposed DHPR tetrads may be stabilized by the strong RyR1-RyR1 interaction. In cardiac muscle, DHPR may not exert inhibition on RyR2s because DHPRs are randomly arranged, without their tetrad correlation to RyR2s (7,8). In addition, RyR2 is more easily activated by Ca^{2+} noise due to its higher sensitivity to the activation of Ca^{2+} (37,38). But the stability of RyR2s still can be achieved if a strong oligomeric interaction also exists between arrayed RyR2s under resting conditions. The modulation of the oligomerization of RyR2s by their functional states is required to be further elucidated.

Second, the activation-induced decrease in RyR1-RyR1 interaction provides insight for understanding the operation of activated RyR1 arrays during E-C coupling. In native RyR1 two-dimensional arrays, activated RyR1s may not de-oligomerize with the support of lipid bilayer. But the interaction between neighboring RyR1s may also decrease accompanying the conformational change(s) with the activation of RyR1s. With the loose association between RyR1s, opened RyR1s would tend to behave more like independent channels. Every RyR1 in the array could then be more freely closed by multiple possible physiological mechanisms, i.e., stochastic closing of RyRs, Ca^{2+}-induced inactivation of RyRs, SR Ca^{2+} depletion, etc. (39–41).

Third, the recovered strong interaction between neighboring closed RyR1s may contribute to the rapid termination of E-C coupling. During E-C coupling, once the neighboring RyR1s in two-dimensional array return from activated state to their resting closed state, the recovered RyR1-RyR1 strong interaction may stabilize them in closed state, efficiently inhibiting the reactivation of these channels. Thus the termination of E-C coupling could be facilitated.

Many proteins are found to cluster in the membrane, but their physiological roles are often obscure (42–44). In the present work, by quantitatively studying RyR1 oligomerization/de-oligomerization within an aqueous system, we have discovered a basic rule that RyR1-RyR1 oligomeric interaction is inversely related to their activation level. These findings provide a new experimental paradigm in our attempts to understand the functional and operational significance of RyR arrays. Furthermore, our experimental paradigm opens the possibility of looking at functional interactions between RyR-interacting SR proteins on the functional and oligomeric state of RyR channels.

We thank Drs. Jerome Parness, Heping (Peace) Cheng, Chunhai Fan, and Haiping Fang for critical comments.

This work was supported by grants from the National Nature Science Foundation of China (grant Nos. NSFC30200051, 10335070, and 10304011), and from the Science & Technology Commission of China (grant Nos. 2002CCA00600 and G1999054001).

REFERENCES

1. Rios, E., and G. Pizarro. 1991. Voltage sensor of excitation-contraction coupling in skeletal muscle. *Physiol. Rev.* 71:849–908.
2. Meissner, G. 1994. Ryanodine receptor/Ca^{2+} release channels and their regulation by endogenous effectors. *Annu. Rev. Physiol.* 56:485–508.
3. Lamb, G. D. 2000. Excitation-contraction coupling in skeletal muscle: comparisons with cardiac muscle. *Clin. Exp. Pharmacol. Physiol.* 27: 216–224.
4. Fill, M., and J. A. Copello. 2002. Ryanodine receptor calcium release channels. *Physiol. Rev.* 82:893–922.
5. Bers, D. M. 2002. Cardiac excitation-contraction coupling. *Nature.* 415:198–205.
6. Franzini-Armstrong, C., and J. Kish. 1995. Alternate disposition of tetrads in peripheral couplings of skeletal muscle. *J. Musc. Res. Cell Motil.* 16:319–324.
7. Franzini-Armstrong, C. 1999. The sarcoplasmic reticulum and the control of muscle contraction. *FASEB J.* 13:S266–S270.
8. Franzini-Armstrong, C., F. Protasi, and V. Ramesh. 1999. Shape, size, and distribution of Ca^{2+} release units and couplons in skeletal and cardiac muscles. *Biophys. J.* 77:1528–1539.
9. Loesser, K. E., L. Castellani, and C. Franzini-Armstrong. 1992. Dispositions of junctional feet in muscles of invertebrates. *J. Muscle Res. Cell Motil.* 13:161–173.
10. Marx, S. O., K. Ondrias, and A. R. Marks. 1998. Coupled gating between individual skeletal muscle Ca^{2+} release channels (ryanodine receptors). *Science.* 281:818–821.
11. Marx, S. O., J. Gaburjakova, M. Gaburjakova, C. Henrikson, K. Ondrias, and A. R. Marks. 2001. Coupled gating between cardiac calcium release channels (ryanodine receptors). *Circ. Res.* 88:1151–1158.
12. Cheng, H., W. J. Lederer, and M. B. Cannell. 1993. Calcium sparks: elementary events underlying excitation-contraction coupling in heart muscle. *Science.* 262:740–744.
13. Wang, S. Q., L. S. Sang, E. G. Lakatta, and H. Cheng. 2001. Ca^{2+} signalling between single L-type Ca^{2+} channels and ryanodine receptors in heart cells. *Nature.* 410:592–596.
14. Wang, S. Q., M. D. Stern, E. Ríos, and H. Cheng. 2004. The quantal nature of Ca^{2+} sparks and in situ operation of the ryanodine receptor array in cardiac cells. *Proc. Natl. Acad. Sci. USA.* 101:3979–3984.
15. Yin, C. C., and F. A. Lai. 2000. Intrinsic lattice formation by the ryanodine receptor calcium-release channel. *Nat. Cell Biol.* 2:669–671.
16. Orlova, E. V., I. I. Serysheva, M. van Heel, S. L. Hamilton, and W. Chiu. 1996. Two structural configurations of the skeletal muscle calcium release channel. *Nat. Struct. Biol.* 3:547–552.
17. Schatz, M., M. Heel, W. Chiu, and S. L. Hamilton. 1999. Structure of the skeletal muscle calcium release channel activated with Ca^{2+} and AMP-PCP. *Biophys. J.* 77:1936–1944.
18. Sharma, M. R., L. H. Jeyakumar, S. Fleischer, and T. Wagenknecht. 2000. Three-dimensional structure of ryanodine receptor isoform three in two conformational states as visualized by cryo-electron microscopy. *J. Biol. Chem.* 275:9485–9491.
19. Pecora, R. 1985. Dynamic Light Scattering: Application of Photon Correlation Spectroscopy. Plenum Press, New York.
20. Johnson, C. S., and D. A. Gabriel. 1994. Laser Light Scattering. Dover Publications, Mineola, New York.
21. Reich, Z., J. J. Boniface, D. S. Lyons, N. Borochov, E. J. Wachtel, and M. M. Davis. 1997. Ligand-specific oligomerization of T-cell receptor molecules. *Nature.* 387:617–620.
22. Hu, X. F., K. Y. Chen, R. Xia, Y. Xu, J. L. Sun, J. Hu, and P. H. Zhu. 2003. Modulation of the interactions of isolated ryanodine receptors of rabbit skeletal muscle by Na^+ and K^+. *Biochemistry.* 42:5515–5521.
23. Lai, F. A., and G. Meissner. 1992. Purification and reconstitution of the ryanodine-sensitive Ca^{2+} release channel complex from muscle sarcoplasmic reticulum. *Methods Mol. Biol.* 13:287–305.
24. Wei, Q. Q., S. F. Chen, X. Y. Cheng, X. B. Yu, J. Hu, M. Q. Li, and P. H. Zhu. 2002. Topography of skeletal muscle ryanodine receptors studied by atomic force microscopy. *J. Vac. Sci. Technol.* B18:636–638.
25. Pessah, I. N., R. A. Stambuk, and J. E. Casida. 1987. Ca^{2+}-activated ryanodine binding: mechanisms of sensitivity and intensity modulation by Mg^{2+}, caffeine, and adenine nucleotides. *Mol. Pharmacol.* 31:232–238.
26. Bers, D. M., C. W. Patton, and R. Nuccitelli. 1994. A practical guide to the preparation of Ca^{2+} buffers. *Methods Cell Biol.* 40:3–29.
27. Lindsay, H. M., R. Klein, D. A. Weitz, M. Y. Lin, and P. Meakin. 1988. Effect of rotational diffusion on quasielastic light scattering from fractal colloid aggregates. *Phys. Rev. A.* 38:2614–2626.
28. Lindsay, H. M., R. Klein, D. A. Weitz, M. Y. Lin, and P. Meakin. 1989. Structure and anisotropy of colloid aggregates. *Phys. Rev. A.* 39:3112–3119.
29. Paul-Pletzer, K., S. S. Palnitkar, L. S. Jimenez, H. Morimoto, and J. Parness. 2001. The skeletal muscle ryanodine receptor identified as a molecular target of [^{3}H]azidodantrolene by photoaffinity labeling. *Biochemistry.* 40:531–542.
30. Coronado, R., J. Morrissette, M. Dukhareva, and D. M. Vaughan. 1994. Structure and function of ryanodine receptors. *Am. J. Physiol. Cell Physiol.* 266:C1485–C1504.
31. Meissner, G., E. Rois, A. Tripathy, and D. A. Pasek. 1997. Regulation of skeletal muscle Ca^{2+} release channel (ryanodine receptor) by Ca^{2+} and monovalent cations and anions. *J. Biol. Chem.* 272:1628–1638.
32. Lamb, G. D. 2000. Excitation-contraction coupling in skeletal muscle: comparisons with cardiac muscle. *Clin. Exp. Pharmacol. Physiol.* 27:216–224.
33. El-Hayek, R., B. Antoniu, J. Wang, S. L. Hamilton, and N. Ikemoto. 1995. Identification of calcium release-triggering and blocking regions of the II–III loop of the skeletal muscle dihydropyridine receptor. *J. Biol. Chem.* 270:22116–22118.
34. Saiki, Y., R. El-Hayek, and N. Ikemoto. 1999. Involvement of the Glu^{724}-Pro^{760} region of the dihydropyridine receptor II–III loop in skeletal muscle-type excitation-contraction coupling. *J. Biol. Chem.* 274:7825–7832.
35. Lamb, G. D., R. El-Hayek, N. Ikemoto, and D. G. Stephenson. 2000. Effects of dihydropyridine receptor II–III loop peptides on Ca^{2+} release in skinned skeletal muscle fibers. *Am. J. Physiol. Cell Physiol.* 279:C891–C905.
36. Lee, E. H., J. R. Lopez, J. Li, F. Protasi, I. N. Pessah, D. H. Kim, and P. D. Allen. 2004. Conformational coupling of DHPR and RyR1 in skeletal myotubes is influenced by long-range allosterism: evidence for a negative regulatory module. *Am. J. Physiol. Cell Physiol.* 286:C179–C189.
37. Copello, J. A., S. Barg, H. Onoue, and S. Fleischer. 1997. Heterogeneity of Ca^{2+} gating of skeletal muscle and cardiac ryanodine receptors. *Biophys. J.* 73:141–156.
38. Fruen, B. R., J. M. Bardy, T. M. Byrem, G. M. Strasburg, and C. F. Louis. 2000. Differential Ca^{2+} sensitivity of skeletal and cardiac muscle ryanodine receptors in the presence of calmodulin. *Am. J. Physiol. Cell Physiol.* 279:724–733.
39. Fabiato, A. 1985. Time and calcium dependence of activation and inactivation of calcium-induced release of calcium from the sarcoplasmic reticulum of a skinned cardiac Purkinje cell. *J. Gen. Physiol.* 85:247–289.

40. Stern, M. D. 1992. Theory of excitation-contraction coupling in cardiac muscle. *Biophys. J.* 63:497–517.

41. Tripathy, A., and G. Meissner. 1996. Sarcoplasmic reticulum luminal Ca^{2+} has access to cytosolic activation and inactivation sites of skeletal muscle Ca^{2+} release channel. *Biophys. J.* 70:2600–2615.

42. Maddock, J. R., and L. Shapiro. 1993. Polar location of the chemoreceptor complex in the *Escherichia coli* cell. *Science.* 259:1717–1723.

43. Shuai, J. W., and P. Jung. 2003. Optimal ion channel clustering for intracellular calcium signaling. *Proc. Natl. Acad. Sci. USA.* 100:506–510.

44. Garrido, J. J., P. Giraud, E. Carlier, F. Fernandes, A. Moussif, M. P. Fache, D. Debanne, and B. Dargent. 2003. A targeting motif involved in sodium channel clustering at the axonal initial segment. *Science.* 300:2091–2094.